Transfected Connexin45 Alters Gap Junction Permeability in Cells Expressing Endogenous Connexin43

Michael Koval, Steven T. Geist, Eileen M. Westphale, Alexandra E. Kemendy, Roberto Civitelli, Eric C. Beyer, and Thomas H. Steinberg

Departments of Medicine, Pediatrics and Cell Biology and Physiology, Washington University School of Medicine, St. Louis, Missouri 63110

Abstract. Many cells express multiple connexins, the gap junction proteins that interconnect the cytosol of adjacent cells. Connexin43 (Cx43) channels allow intercellular transfer of Lucifer Yellow (LY, MW = 443 D), while connexin45 (Cx45) channels do not. We transfected full-length or truncated chicken Cx45 into a rat osteosarcoma cell line ROS-17/2.8, which expresses endogenous Cx43. Both forms of Cx45 were expressed at high levels and colocalized with Cx43 at plasma membrane junctions. Cells transfected with full-length Cx45 (ROS/Cx45) and cells transfected with Cx45 missing the 37 carboxyl-terminal amino acids (ROS/Cx45tr) showed 30–60% of the gap junctional conductance exhibited by ROS cells. Intercellular transfer of three negatively charged fluorescent reporter molecules was examined. In ROS cells, microinjected LY was transferred to an average of 11.2 cells/injected cell, while dye transfer between ROS/Cx45 cells was reduced to 3.9 cells. In contrast, ROS/Cx45tr cells transferred LY to >20 cells. Transfer of calcein (MW = 623 D) was also reduced by ~50% in ROS/Cx45 cells, but passage of hydroxycoumarin carboxylic acid (HCCA; MW = 206 D) was only reduced by 35% as compared to ROS cells. Thus, introduction of Cx45 altered intercellular coupling between cells expressing Cx43, most likely the result of direct interaction between Cx43 and Cx45. Transfection of Cx45tr and Cx45 had different effects in ROS cells, consistent with a role of the carboxyl-terminal domain of Cx45 in determining gap junction permeability or interactions between connexins. These data suggest that coexpression of multiple connexins may enable cells to achieve forms of intercellular communication that cannot be attained by expression of a single connexin.

Gap junctions are a complex of transmembrane proteins that form membrane pores at contact points between cells. Gap junction channels allow the passage of ions and small aqueous molecules from the cytoplasm of one cell to another (for reviews see references 2, 13, 31). A functional gap junction channel consists of two plasma membrane hemichannels, one in each cell, composed of hexamers of transmembrane proteins known as connexins. A number of connexin proteins have been identified with molecular masses in the range of 26–56 kD (6, 40). The role for connexin multiplicity is unknown at present. Electrophysiologic studies have revealed that connexins differ in unitary conductances and voltage sensitivity (1, 33, 38, 39), while dye transfer has been used to show that different connexins form channels with different molecular permeabilities (7, 32, 37).

Many cells express more than one connexin. Differential expression of connexins during development (7, 10, 36), tissue regeneration (18), and oncogenesis (21, 34) suggests that alterations of gap junction composition are important for cell regulation. Brisette et al. have correlated developmentally regulated changes in connexin expression in keratinocytes with selective alterations in the intercellular transfer of cytidine triphosphate and methionine (7).

We have found using two rat osteoblastic cell lines that two gap junction proteins, connexin43 (Cx43[1]; α_1) and connexin45 (Cx45; α_6), form channels with different molecular permeability. ROS-17/2.8 (ROS) cells express Cx43 at the cell surface and are able to efficiently transfer microinjected Lucifer yellow (LY) through gap junctions (32). In contrast, UMR 106-01 (UMR) cells, express predominantly Cx45 at the plasma membrane and poorly transfer LY (27, 32). However, small ions can pass through UMR gap junctions, as demonstrated by intercellular currents measured with the double cell patch clamp technique

Please address all correspondence to M. Koval, Department of Medicine, Washington University School of Medicine, Campus Box 8051, 660 S. Euclid Avenue, St. Louis, MO 63110. Tel.: (314) 362-6606. Fax: (314) 362-9230.

1. *Abbreviations used in this paper*: calcein-AM, calcein-acetoxymethylester; Cx43, connexin43; HCCA, hydroxycoumarin carboxylic acid; LY, Lucifer yellow; ROS, ROS-17/2.8.

(32, 37). Increasing Cx43 expression by hormone treatment increased LY dye transfer in a number of osteoblastic cell models (10, 11, 26, 28).

Consistent with these observations, we found that transfection of Cx43 into UMR cells confers the ability to transfer LY by gap junctions, but overexpression of chicken Cx45 by UMR cells has no effect on intercellular LY transfer (32). This observation also suggests that chicken and mammalian Cx45 have similar permeability (23, 37).

Since LY can diffuse through Cx43 channels, but not through Cx45 channels, we wanted to determine whether introduction of Cx45 into ROS cells would alter intercellular communication. This enabled us to examine consequences of expressing multiple connexins in a single cell and to determine whether these two connexins were capable of interaction. ROS cells were stably transfected with either full-length Cx45 (ROS/Cx45) or a truncated Cx45 with the 37 carboxyl-terminal amino acids removed (ROS/Cx45tr), and then the gap junction permeability in these cells was examined using fluorescent reporter molecules in the 200–650-D size range. We found that transfected Cx45 altered intercellular communication between ROS cells, suggesting that native Cx43 was interacting with Cx45. This suggests that the expression of multiple connexins may be a mechanism for the control of gap junction–mediated intercellular communication.

Materials and Methods

Cells and DNA Constructs

ROS 17/2.8 cells were cultured in MEM (No. 11095-056, GIBCO BRL, Gaithersburg, MD) containing 10% heat-inactivated bovine calf serum (Hyclone, Logan, UT), 2 mM glutamine, 1 mM sodium pyruvate and 1% nonessential amino acids (GIBCO BRL), 5 u/ml penicillin, and 5 μg/ml streptomycin (MEM+BCS).

Chicken Cx45 is over 80% identical to the corresponding mammalian gene product at the amino acid level. Chicken Cx45 cDNA was isolated as previously described (3). To create a truncated form of Cx45 (Cx45tr), Cx45 cDNA in Bluescript KS was first amplified by PCR using a sense oligonucleotide: 5′-GAGGT CGACG GTATC GATAA GCTTG-3′ and an anti-sense oligonucleotide: 5′-GAGCT GCTGA ATTCG GTTGT TTTGG TTGTT CTACG CCTGG AT-3′, which replaced the codon corresponding to amino acid 357 with a stop codon and added an additional EcoRI site. The resulting PCR product was digested with EcoRI and then inserted into the EcoRI site of expression vector pSFFVneo (9). Insertion of full-length Cx45 in pSFFVneo was previously described (36).

ROS cells were transfected with these pSFFVneo constructs using lipofectin (GIBCO BRL). Cells were selected by culturing in medium containing 0.5 μg/ml geneticin (GIBCO BRL), and then plated at limiting dilution to obtain single cell colonies which were screened for Cx45 or Cx45tr expression by RNA blot (see below).

RNA Blots

Total cellular RNA was isolated using guanidinium isothiocyanate, resolved on formaldehyde-agarose gels and transferred to nylon membranes. The membranes were hybridized to ^{32}P-labeled chicken Cx45 cDNA probes (3) in 0.75 M sodium phosphate, 1% SDS, 100 μg/ml salmon sperm DNA at 65°C and washed under high stringency conditions using 30 mM sodium phosphate, 1% SDS, 65°C. Cx45 mRNA was detected by autoradiography. The blots were stripped and rehybridized with a human γ-actin cDNA probe to assess the total mRNA added to the gel.

Immunofluorescence

Rabbit polyclonal antisera to Cx43 and Cx45 were generated from synthetic peptides as previously described (3, 4, 19). Cells were cultured on glass coverslips 1–3 d before treatment. The cells were fixed in methanol/acetone (1:1) for 2 min at room temperature and washed with PBS. For single-label experiments, cells were incubated in PBS containing either anti-Cx43 or anti-Cx45 antiserum for 45 min at room temperature. The cells were then washed, labeled with rhodamine-conjugated goat anti–rabbit IgG (Boehringer Mannheim, Indianapolis, IN), washed and viewed by fluorescence microscopy.

ROS/Cx45 and ROS/Cx45tr cells were double labeled in a similar manner, except that cells were treated with PBS containing monoclonal anti-Cx43 IgG (No. 03-6900; Zymed Laboratories, South San Francisco, CA) before treatment with polyclonal anti-Cx45 antiserum. Anti-Cx43 was visualized by confocal microscopy (BioRad Labs., Richmond, CA) with Texas red–conjugated goat anti–mouse IgG (Cappel, Durham, NC) and anti-Cx45 was visualized with FITC-conjugated goat anti–rabbit IgG (Cappel).

Alkali Solubilization and Immunoblot

Alkali-insoluble material was isolated using a procedure modified from Hertzberg (15). Cells were scraped from two confluent 100-mm culture dishes into PBS, centrifuged, resuspended in 1 ml of 1 mM $NaHCO_3$ containing protease and phosphatase inhibitors (1 mM PMSF, 1 mM Na_2VO_4, 10 mM NaF, 2 μg/ml leupeptin, 1 μg/ml pepstatin) at 4°C, and then made alkaline with 22 μl of 1 M NaOH. The suspension was sonicated at 4 W for 30 s, incubated on ice for 50 min, and then centrifuged in a Beckman Optima TL ultracentrifuge at 30,000 *g* for 30 min. The resulting pellet was resuspended in 40 μl sample buffer (50 mM Tris, 0.01% (vol/vol) β-mercaptoethanol, 10% (vol/vol) glycerol, 2% (wt/vol) SDS, 10 mg/ml bromophenol blue, pH 6.7), heated to 68°C for 10 min, and the proteins were resolved by SDS-PAGE using standard methods and 10% polyacrylamide gels (14). The proteins were then electrophoretically transferred to PVDF membranes (transfer buffer: 50 mM tris, 380 mM glycine, 0.025% [wt/vol] SDS, 20% MeOH), blocked with blotto (40 mM Tris, 5% (wt/vol) Carnation powdered milk, 0.1% (vol/vol) Tween-20) for 1 h at room temperature and incubated overnight with mixing with either anti-Cx43 IgG or anti-Cx45 antiserum diluted into blotto. The membranes were then washed, incubated for 1 h with horseradish peroxidase–conjugated goat anti–rabbit IgG (Tago, Burlingame, CA) diluted 1:8,000 into blotto, washed, and peroxidase activity was detected using ECL (Amersham International, Buckinghamshire, UK).

Flow Cytometry

Flow cytometry was used to assess intercellular communication (34). One day before assay, cells were harvested with trypsin/EDTA. Approximately one third of these cells were replated for use the next day as donor cells at 10^7 cells/100-mm tissue culture dish (Sarstedt, Newton, NC). The rest of the cells (2×10^7) were labeled with a nontransferrable dye, PKH-26 (17), using reagents from Sigma Chem. Co. (St. Louis, MO) to produce acceptor cells. The cells were washed with PBS, resuspended in 1 ml of diluent C and then added to 1 ml of diluent C containing 4 μM PKH-26. The cells were incubated at room temperature for 3 min, and then 2 ml BCS was added to quench the reaction. After a 1 min incubation, 4 ml MEM+BCS was added to the tube, the cells were centrifuged, washed 3× with MEM+BCS and then cultured overnight in two 100 mm tissue culture dishes. Donor cells were labeled with the calcein-acetoxymethylester (calcein-AM; Molecular Probes, Eugene, OR). Cells in culture dishes were washed, incubated at 37°C for 15 min with 5 ml of MEM+BCS containing 5 μl of 1,000× calcein-AM stock solution (1 mg/ml in EtOH), and then further washed with MEM+BCS. Both donor and acceptor cells were harvested by trypsinization, washed, and resuspended to 2.5×10^6 cells/ml in MEM+BCS. The cells were then added to 35 mm tissue culture dishes (Falcon brand, Becton Dickinson, Lincoln Park, NJ) at varying acceptor/donor (A/D) ratios (2.5×10^6 total cells/dish). After incubation in a CO_2 incubator for 5 h at 37°C, the cells were harvested by trypsinization, resuspended in 3 ml MEM+BCS and analyzed by flow cytometry using a Coulter EPICS/XL (Irving, TX). Calcein was detected with channel 1 (525 nm BP) and PKH-26 was detected with channel 2 (575 nm BP).

Electrophysiological Measurements

Junctional conductances (g_j) were determined using the double whole cell patch clamp technique as previously described (35, 37). Patch pipettes were fabricated from Boralex micropipette glass (Rochester Scientific Co., Rochester, NY) and fire-polished to a tip diameter of ≤1 μm. Tip resistances varied between 2–5 MΩ. Patch electrodes were coated before use with Sylgard (Dow Corning, Midland, MI) to reduce electrode capaci-

tance. The pipettes contained a solution of 3 mM ATP, and 3 mM phosphocreatine, 120 mM K glutamate, 15 mM NaCl, 1 mM KH_2PO_4, 4 mM $MgCl_2$, 0.1 mM ethylene glycol-bis-(β-aminoethyl ether)-N,N,N′,N′-tetraacetic acid (EGTA), 10 mM N-2-hydroxyethylpiperazine-N′-2-ethane-sulfonic acid (Hepes), pH 7.4.

During patch-clamp experiments, the cells were in a balanced salt solution containing 142 mM NaCl, 1.3 mM KCl, 0.8 mM $MgSO_4$, 0.9 mM NaH_2PO_4, 1.8 mM $CaCl_2$, 5.5 mM dextrose, 10 mM Hepes, pH 7.4, at room temperature. Whole cell currents were obtained with two Axopatch 200A integrating current-voltage clamp amplifiers (Axon Instruments, Inc., Foster City, CA). The pipette/cell seals were in the giga-ohm range and voltages were corrected for access resistance.

To determine g_j, the cells were first clamped to −40 mV, and then the membrane voltage of the second cell was pulsed to +140 mV in 20 mV increments at a frequency of 2 kHz. Each pulse was 5 s in duration and pulses were separated by a 2 s return to the holding voltage. Data were digitized at 4 kHz using pCLAMP software (version 6.0.1; Axon Instruments, Foster City, CA) and g_j was calculated from transjunctional current measurements.

Dye Transfer by Microinjection

Cells were cultured on glass coverslips 1–3 d before microinjection experiments. The coverslips were mounted in a tissue chamber (Medical Systems Corp., Greenvale, NY) on an epifluorescence microscope, covered with culture medium containing 2.5 mM probenecid and maintained at 37°C in a 5% CO_2 atmosphere. Cells were microinjected with solutions containing either 34 mg/ml Lucifer yellow CH (LY; MW = 443 g/mol), 20 mg/ml calcein (MW = 623 g/mol), 20 mg/ml calcein blue (MW = 321 g/mol) or 10 mg/ml hydroxycoumarin carboxylic acid (HCCA; MW = 206 g/mol) (all from Molecular Probes) using 1100–1200 psi applied for 0.2–0.3 s. 2–5 min after injection, the extent of intercellular dye transfer was determined by recording the number of adjacent cells containing dye that were visualized using suitable optics with a CCD camera with an image intensifier (Dage MTI, Michigan City, IN) and an image processing system (Georgia Instruments, Roswell, GA).

In some cases cells were microinjected with a neutral aqueous solution containing both calcein and HCCA at 6.7 mg/ml. We used 400DCLP dicroic and 510WB40 emission filters (Omega Optics, Brattleboro, VT) combined with a monochromator excitation source (CVI Laser Corp, Alberquerque, NM) to view HCCA (388 nm) or calcein (465 nm) with minimal crosstalk.

Results

Transfection of Cx45 Constructs into ROS Cells

ROS cells express Cx43 at the cell surface (Fig. 2 *a*) and do not express Cx45 (Fig. 1) as previously described (11, 32). We stably transfected ROS cells with two chicken Cx45 constructs, either full-length Cx45 cDNA (ROS/Cx45) or a truncated Cx45 construct which encodes a form of Cx45 with 37 amino acids deleted from the cytoplasmic COOH-terminal domain (ROS/Cx45tr). G418-resistant, single cell colonies were selected by limiting dilution, and we identified ROS/Cx45 and ROS/Cx45tr cell lines that showed transfected mRNA expression (Fig. 1). Cx45 mRNA appeared as a doublet, which may reflect alternative polyadenylation or splicing as a result of sites in both the expression vector and cDNA (36).

We next examined the expression and intracellular distribution of Cx43 and Cx45 proteins in these cells. By indirect immunofluorescence, we found Cx43 largely localized to areas of intercellular contact (Fig. 2), characteristic of gap junction plaques. In transfected cells, both truncated and full-length Cx45 showed a similar intracellular distribution to that of Cx43. Examination of double-labeled cells by confocal fluorescence microscopy confirmed that Cx43 and Cx45 were extensively colocalized (Fig. 3). Thus, at the morphological level, both the full-length and truncated forms of Cx45 were transported by the cell to sites where they have the potential to participate in intercellular communication. Also, the intracellular distribution of Cx43 in these cells did not appear to be altered by expression of Cx45 or Cx45tr.

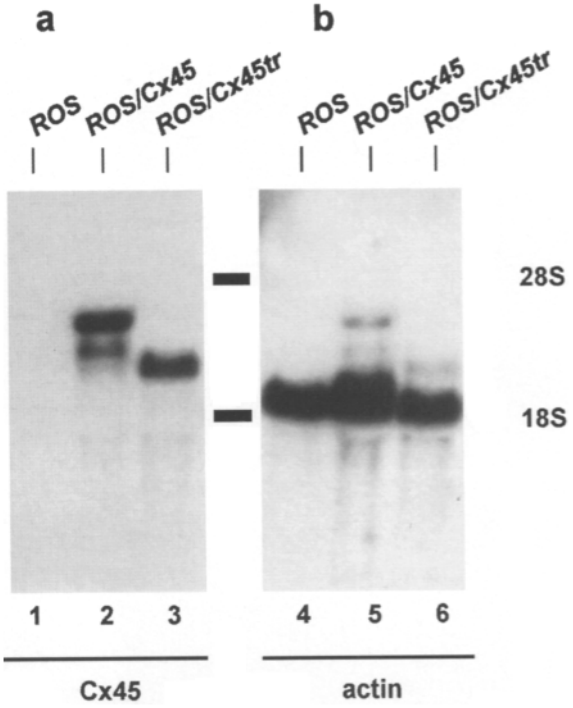

Figure 1. Northern blot analysis of Cx45 mRNA. Total RNA was isolated from either ROS (lanes *1* and *4*), ROS/Cx45 cells (lanes *2* and *5*), or ROS/Cx45tr (lanes *3* and *6*) and subjected to agarose gel electrophoresis, transferred to membranes, and then probed for mRNA corresponding to Cx45 (*a*). Note the lack of Cx45 mRNA in ROS cells (lane *1*). (*b*) The membranes were then stripped and reprobed for actin as a control for mRNA loading. Dashes correspond to 28s and 18s rRNA.

To further examine Cx43 and Cx45 expression, preparations enriched for gap junction plaques were made by alkaline extraction of cells hydrolyzed in a hypotonic bicarbonate buffer (15). Plaque-enriched pellets from ROS, ROS/Cx45, and ROS/Cx45tr cells were resolved by SDS-PAGE and analyzed by immunoblotting. As shown in Fig. 4, all three cell types showed Cx43 associated with the insoluble pellet. Note that Cx45 was also associated with the alkali-insoluble material (Fig. 4).

All three cell lines contained immunoreactive Cx43 that appeared as a doublet at 40 and 42 kD, suggesting Cx43 phosphorylation by transfected and untransfected cells (24, 25). ROS/Cx45 and ROS cells produced equivalent amounts of alkali-insoluble Cx43. The ratio of alkali-insoluble Cx43 produced by ROS/Cx45 cells to that produced by ROS cells was 1.0 ± 0.3 (n = 8), as determined by densitometric measurement of immunoblots. We also found that ROS/Cx45tr cells expressed 1.7 ± 0.6 (n = 4)-fold more alkali-insoluble Cx43 than ROS cells. The expression of Cx45tr relative to Cx43 by ROS/Cx45tr cells (Cx45tr:Cx43 ratio = 0.29 ± 0.14 [n = 3]) was comparable to ROS/Cx45 cells (Cx45:Cx43 ratio = 0.22 ± 0.01 [n = 3]) as determined by densitometry. Similar results were ob-

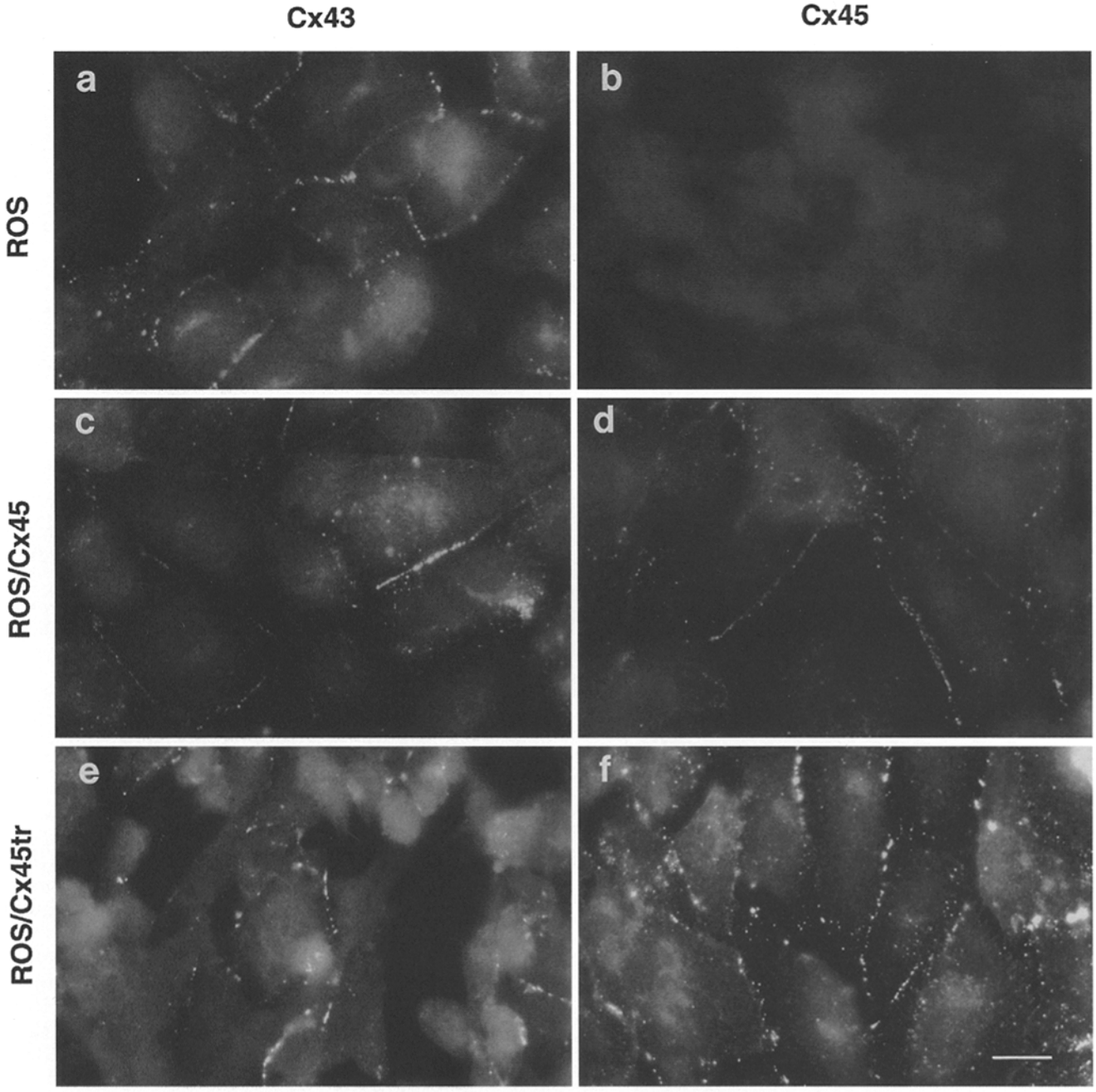

Figure 2. Intracellular distribution of connexins in osteoblast cells. ROS (*a* and *b*), ROS/Cx45 (*c* and *d*), or ROS/Cx45tr (*e* and *f*) cells were cultured on glass coverslips, fixed, permeabilized, and then incubated with rabbit IgG to either Cx43 (*a*, *c*, and *e*) or Cx45 (*b*, *d*, and *f*) diluted in PBS for 1 h at room temperature. The cells were then washed, labeled with Texas red–conjugated goat anti–rabbit IgG and photographed. Note the lack of Cx45 labeling of untransfected ROS cells (*b*). Cx43 and, in transfected cells, Cx45 appear largely in bright, punctate regions located where cells come into close apposition which correspond to gap junctions. Bar, 20 μm.

tained by immunoprecipitation of total cellular extracts of [^{35}S]methionine labeled Cx43 and Cx45 (not shown).

FACS Assays for Dye Transfer

To determine whether expression of Cx45 or Cx45tr altered intercellular communication between ROS cells, cell coupling was assessed using a FACS assay developed by Tomasetto et al. (34). Cells were harvested and divided into two populations. One set of cells was labeled with a permanent, lipophilic dye, PKH-26. The second set was labeled with calcein-AM which diffuses across the plasma membrane into the cytosol, where it is hydrolyzed to free calcein and can act as a reporter for aqueous transfer between cells. The two sets of cells were cultured together for 5 h to allow transfer of calcein from donor cells to PKH-26–labeled acceptor cells, reharvested, and then the number of double-labeled cells was determined by flow cytometry.

Differences between the cell types were revealed by plating cells at increasing acceptor/donor (A/D) ratio. In

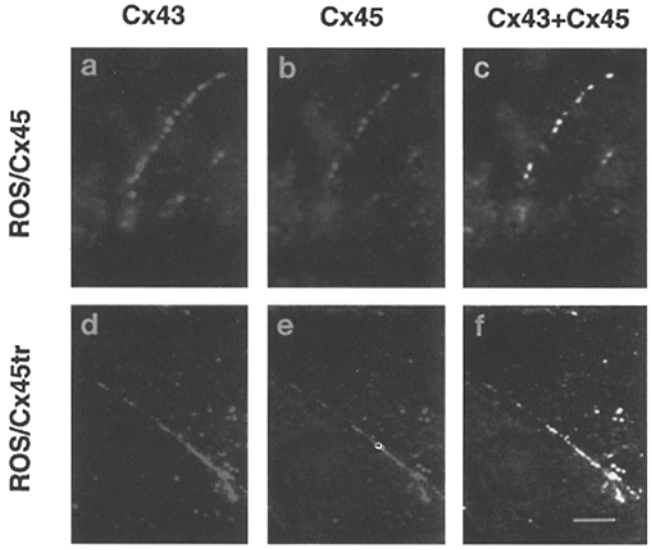

Figure 3. Confocal immunofluorescence microscopy of Cx43 and Cx45. ROS/Cx45 (*a–c*) or ROS/Cx45tr (*d–f*) cells were cultured on glass coverslips, fixed, permeabilized, incubated with monoclonal mouse IgG to Cx43, washed then incubated with affinity-purified rabbit anti-Cx45 IgG. The cells were then washed, labeled with Texas red–conjugated goat anti–mouse IgG and FITC-conjugated goat anti–rabbit IgG and images were obtained using optics suitable for Texas red (Cx43; *a* and *d*) and FITC (Cx45, *b*; Cx45tr, *e*). Note the extensive colocalization of Cx43 and the Cx45 constructs. This was confirmed by computing the logical "and" of images of the intracellular distribution of Cx43 and Cx45 (*c*) or Cx43 and Cx45tr (*f*), where high intensity pixels correspond to pixels with high levels of Cx43 and Cx45 labeling. Bar, 5 μm.

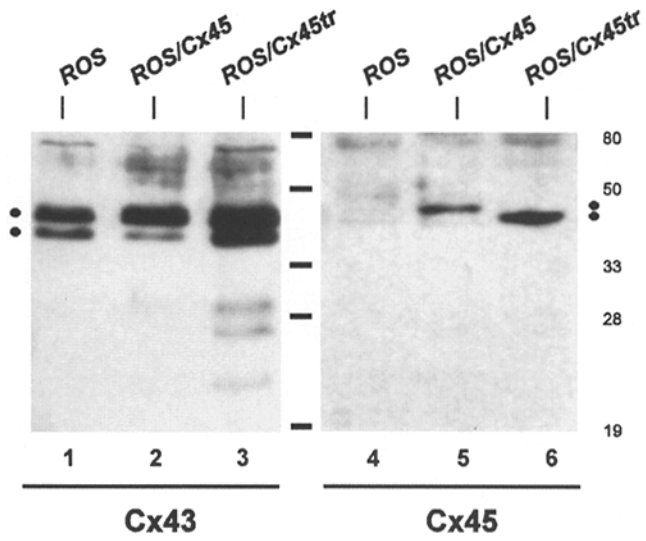

Figure 4. Western immunoblot analysis of alkali-insoluble material enriched for gap junctions. Alkali-insoluble material was prepared as described in Materials and Methods from ROS (lanes *1* and *4*), ROS/Cx45 (lanes *2* and *5*), or ROS/Cx45tr (lanes *3* and *6*) cells, resolved by SDS-PAGE, transferred to a PVDF membrane and probed with IgG to either Cx43 (lanes *1–3*) or Cx45 (lanes *4–6*). Note the presence of Cx45 (lane *5*) and Cx45tr (lane *6*) in the alkali insoluble pool, consistent with localization of these proteins in gap junction plaques. Specific bands are denoted by dots and dashes correspond to M_r markers of 80.0, 49.5, 32.5, 27.5, and 16.6 kD.

all three cell types examined, the amount of calcein transfer decreased with increasing A/D ratio (Figs. 5 and 6). However, ROS/Cx45 cells showed a much more dramatic decrease in dye coupling. At the highest A/D ratio examined, where dye transfer is most dependent on second order transfer of calcein between cells, ROS/Cx45 showed much less dye transfer than either ROS or ROS/Cx45tr cells (Figs. 5, *j–l* and 6). ROS and ROS/Cx45tr cells showed comparable intercellular calcein transfer during the 5-h incubation period as assessed by this FACS method.

We also examined dye transfer using the FACS assay in heterogeneous cell cultures at A/D ratio of 20:1 (Fig. 6 *c*). Both ROS/Cx45 and ROS/Cx45tr cells were as effective as ROS donor cells, when cocultured with ROS acceptor cells (Fig. 6 *c*). However, using ROS donor cells, ROS/Cx45 acceptor cells showed significantly less dye transfer than ROS/Cx45tr cells, further confirming that full-length chicken Cx45 reduced the ability of ROS cells to transfer calcein between cells. This also was consistent with results from homogeneous cultures, where second order dye transfer between acceptor cells was the dominant component in determining the extent of double labeling at this ratio.

Gap Junctional Conductance

We used the double-cell patch clamp method to measure g_j (see Materials and Methods). The current-voltage relation was linear in the range ± 60 mV for all three cell types (not shown). All three cell types had different g_j (ROS; g_j = 32.3 ± 4.5 nS [n = 7], ROS/Cx45; 19.8 ± 2.1 nS [n = 7], ROS/Cx45tr 9.2 ± 1.2 nS [n = 5]). By Student's two-tailed t test (29), all three g_j values were significantly different from the other two ($P < 0.001$). Values for whole cell gap junctional conductance did not correlate with the ability for the cells to transfer calcein as determined by the FACS assay. Thus, the differences in calcein transfer measured by FACS were not due only to an overall decrease in gap junctional intercellular communication, since ROS/Cx45 cell pairs had higher g_j than ROS/Cx45tr cells.

Measurement of Molecular Permeability by Transfer of Microinjected Dyes

To further examine intercellular communication, cell coupling was assessed by visualization of the transfer of microinjected fluorescent dyes between cells (Fig. 7). Untransfected ROS cells transferred microinjected LY to an average of 11.2 ± 6.6 (n = 59) cells/microinjected cell. In contrast, dye-transfer between ROS/Cx45 cells was reduced to 3.9 ± 3.7 (n = 74). Two other ROS/Cx45 clones also showed comparable reduction in LY dye transfer (4.8 ± 2.7 [n = 40], 4.0 ± 3.2 [n = 40]). The difference in the extent of LY dye transfer observed for ROS and ROS/Cx45 cells was statistically significant ($P < 0.001$) as assessed by the nonparametric Wilcoxon/Mann-Whitney U test (29). Cx45tr had the opposite effect on dye-coupling between cells (Fig. 7).

ROS/Cx45tr cells showed enhanced transfer of LY with typically greater than 25 cells coupled to the microinjected

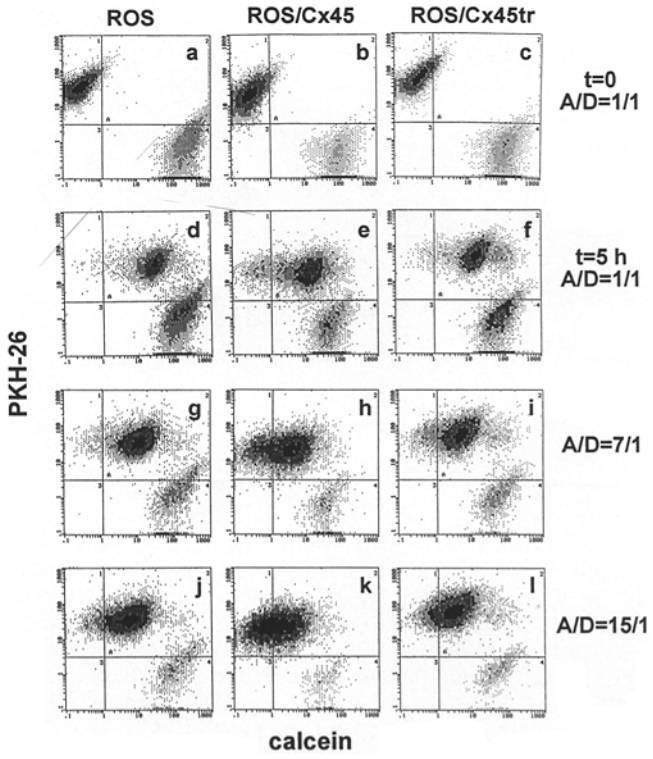

Figure 5. Flow cytometric assay of intercellular dye transfer. Donor cells labeled with calcein-AM and acceptor cells labeled with PKH-26 were cocultured as described in Materials and Methods. (*a*, *d*, *g*, and *j*) ROS cells; (*b*, *e*, *h*, and *k*) ROS/Cx45 cells; and (*c*, *f*, *i*, and *l*) ROS/Cx45tr cells. (*a–c*) Donor and acceptor cells mixed just before FACS analysis. Cells containing PHK-26 alone appeared in quadrant 1, while cells labeled with calcein alone were in quadrant 4. In the other panels, cells were cocultured for 5 h at donor-acceptor ratios of roughly 1:1 (*d–f*), 1:7 (*g–i*), or 1:15 (*j–l*) before harvesting and FACS analysis (see Fig. 6). Double-labeled acceptor cells that had received calcein appear in quadrant 2. ROS/Cx45 show significantly fewer double-labeled cells (*h* and *k*) than comparably treated ROS (*g* and *j*) or ROS/Cx45tr (*i* and *l*) cells.

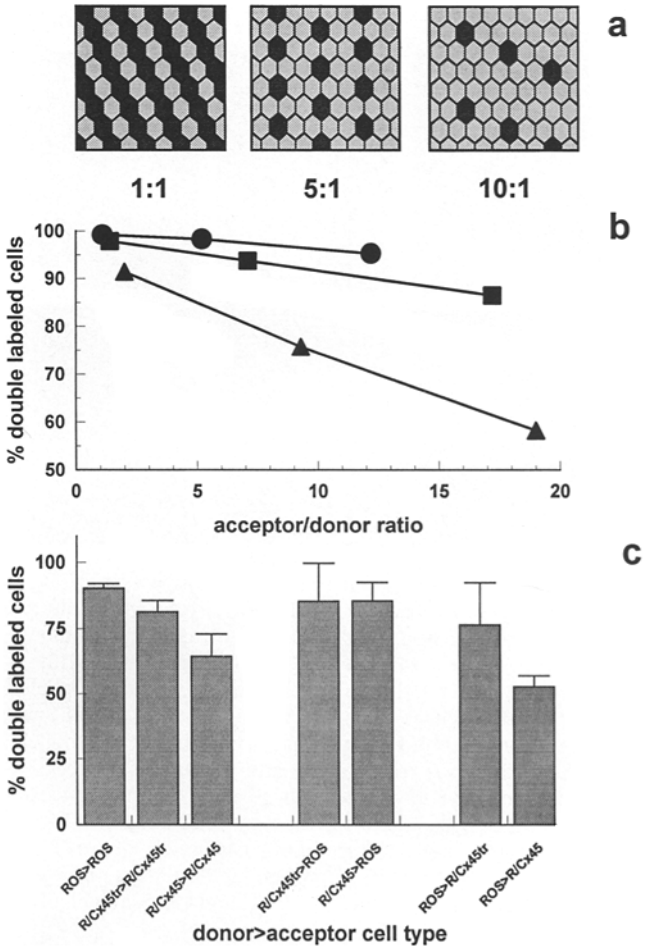

Figure 6. Expression of Cx45 decreases intercellular communication in ROS/Cx45 cells. (*a*) Schematic showing cells plated at acceptor:donor (A/D) ratios of 1:1, 5:1, and 10:1, where donor cells are dark and acceptor cells are light. This assumes that each cell is surrounded by six neighbors and is for illustrative purposes only. Note that A/D ratios on the order of 10:1 or 20:1 are required to get a monolayer where acceptor cells are in direct contact with a maximum of one donor cell. (*b*) The percent of double-labeled cells was calculated from FACS data (Fig. 5, *d–l*) using the number of cells in quadrant 2 divided by the total number of PKH-26–labeled cells analyzed. A/D ratios were determined as the ratio of the number of cells in quadrants 1 and 2 to the number of cells in quadrants 3 and 4. ROS (●), ROS/Cx45tr (■), and ROS/Cx45 (▲) cells were examined. (*c*) Acceptor cells labeled with PKH-26 were cocultured for 5 h at A/D of 20:1 with various donor cells as indicated on the X-axis label, and then harvested and analyzed by FACS as described above. Bars represent the average of five experiments ± SE.

cell. This enhanced level of cell coupling by ROS/Cx45tr cells differed from results obtained with the FACS assay and is likely to reflect differences between these two methods of analyzing intercellular communication (see Discussion).

To determine differences in the molecular permeability of gap junctions in ROS and ROS/Cx45 cells, we examined the intercellular transfer of two negatively charged fluorescent dyes of different size calcein, and HCCA. As shown in Fig. 8, *c* and *d*, ROS/Cx45 cells showed reduced transfer of microinjected calcein, consistent with results obtained with LY (Fig. 7). Using the Kolmogorov-Smirnov test (29, 11), we confirmed that the distributions obtained with calcein and LY were equivalent for the same cell type. Intercellular transfer of calcein for ROS (8.3 ± 5.2 coupled cells/microinjected cell, $n = 41$) and ROS/Cx45 (4.2 ± 3.4, $n = 50$) were significantly different ($P < 0.001$).

In contrast, transfer of a smaller fluorescent dye, HCCA, was less attenuated in cells expressing full-length Cx45 (Fig. 8, *a* and *b*). The distribution of intercellular transfer of HCCA by ROS cells (9.2 ± 4.6, $n = 55$) was comparable to that obtained with calcein and LY in ROS cells, as verified by the Kolmogorov-Smirnov test. The extent of HCCA transfer by ROS/Cx45 cells (5.9 ± 3.8, $n = 43$) was significantly different from the extent of HCCA transfer by ROS cells ($P < 0.01$). However, we also confirmed that the amount of HCCA transfer by ROS/Cx45 cells was significantly different than the extent of either LY or calcein transfer by ROS/Cx45 cells, using the Wilcoxon/Mann-Whitney U test ($P < 0.02$). Similar results were obtained with calcein blue, which closely resembles HCCA, where

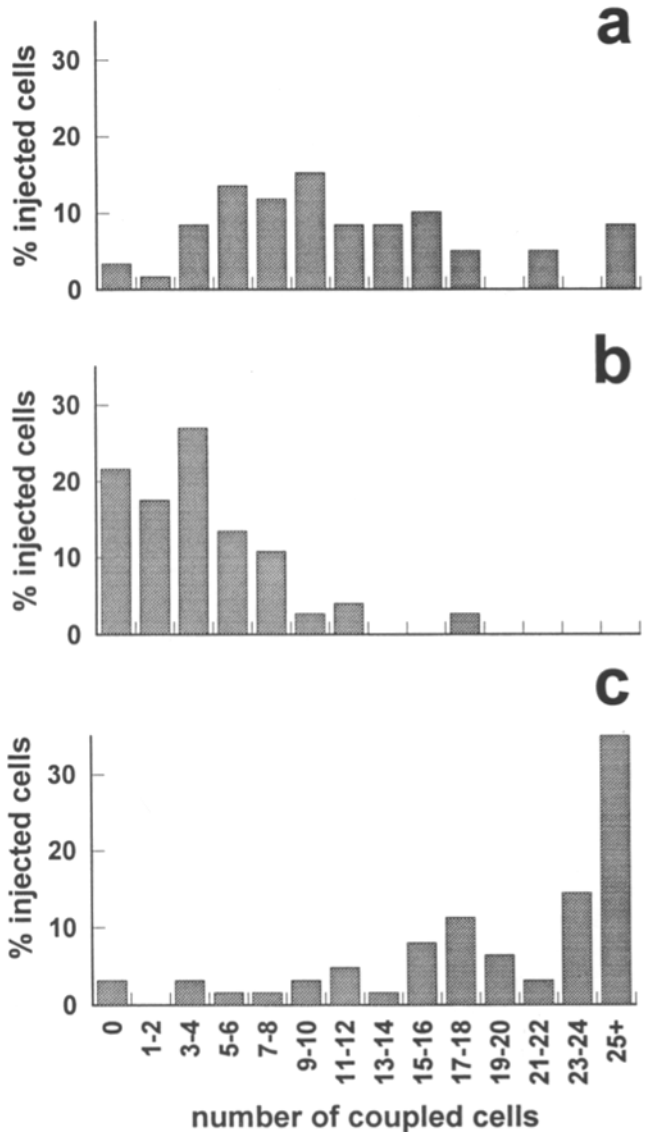

Figure 7. Intercellular transfer of microinjected Lucifer yellow is altered by expression of Cx45 constructs. Dye transfer between ROS (*a*), ROS/Cx45 (*b*), or ROS/Cx45tr (*c*) cells cultured on glass coverslips was assessed by the direct visualization of the movement of microinjected LY using fluorescence microscopy. For each microinjection event, the number of coupled cells was determined as the number labeled by LY. The number of microinjections were 59, 78, and 41 for ROS, ROS/Cx45, and ROS/Cx45tr cells, respectively.

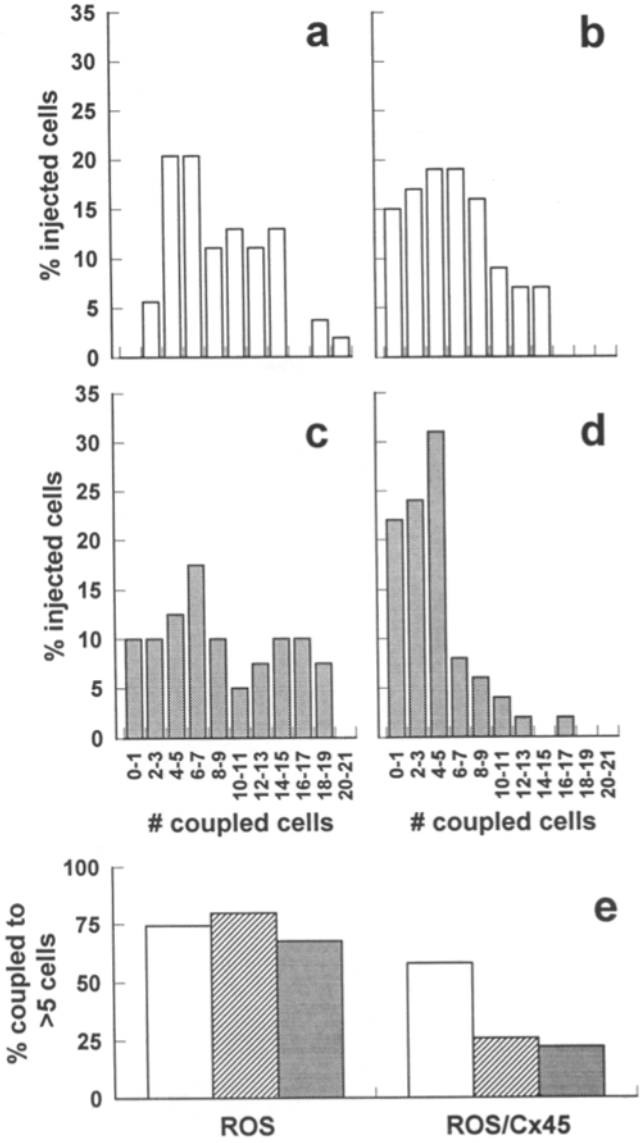

Figure 8. ROS/Cx45 cells show differential intercellular transfer of different sized fluorescent dyes. Dye transfer between ROS (*a* and *c*) or ROS/Cx45 (*b* and *d*) cells cultured on glass coverslips was assessed by the direct visualization of the movement of microinjected calcein (*dark bars*; *c* and *d*) or HCCA (*light bars*; *a* and *b*) using fluorescence microscopy. For each microinjection event, the number of coupled cells was determined as the number labeled by a given fluorescent dye. The number of calcein microinjections were 41 and 50, for ROS and ROS/Cx45, respectively, and for HCCA were 55 and 43 for ROS and ROS/Cx45. (*e*) Intercellular transfer for HCCA (*light bars*), LY (*stippled bars*), and calcein (*dark bars*), expressed as the percentage of microinjections showing coupling to six or more cells. ROS cells transferred all of these dyes in a comparable manner, as opposed to ROS/Cx45 cells which had more reduced transfer of calcein and LY than transfer of HCCA.

ROS/Cx45 cells showed calcein blue transfer to 6.3 ± 3.8 cells/injected cell (n = 20).

To show the relationship between reporter molecule size and the amount of second-order cell coupling, we expressed these microinjection data as a percentage of total microinjections where the dye was passed to six or more cells (Fig. 8 *c*). While ROS cells showed little difference in the ability to transfer these three differently sized dyes, ROS/Cx45 cells were much more effective in the extended transfer of the smallest dye, HCCA, as compared to the two larger dyes. We further confirmed this visually by microinjecting a solution containing both calcein and HCCA into ROS and ROS/Cx45 cells which enabled us to simultaneously examine transfer of these dyes in the same monolayer (Fig. 9). Consistent with the quantitative analysis of dye transfer described above, ROS/Cx45 cells preferentially transferred HCCA, while transfer of calcein was more restricted.

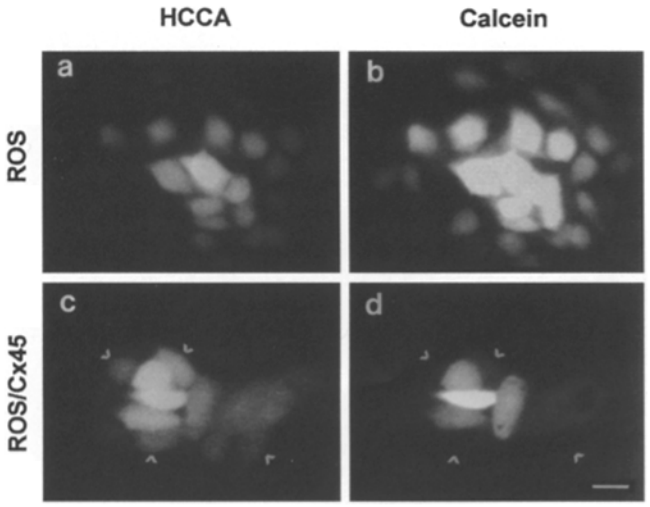

Figure 9. Comicroinjection of calcein and HCCA. ROS (*a* and *b*) or ROS/Cx45 (*c* and *d*) cells were microinjected with a solution containing a mixture of calcein and HCCA and visualized by fluorescence microscopy as described in Materials and Methods. ROS cells showed equivalent dye transfer for both calcein (*b*) and HCCA (*a*), while ROS/Cx45 cells had preferential transfer of the smaller dye, HCCA (*c*), to some cells (*arrowheads*). Bar, 40 μm.

Discussion

In this paper we used three differently sized fluorescent reporter molecules to show that the expression of full-length chicken Cx45 decreased molecular permeability of intercellular communication between ROS cells. All of the probes were efficiently transferred by ROS cells, where gap junction channels were composed of Cx43 alone. In ROS/Cx45 transfectants, intercellular transfer of LY and calcein were reduced by ~50–65%, while transfer of a smaller dye, HCCA, was decreased by ~35%. The probes used in this study all have net negative charge. Previous electrophysiological studies on Cx45 gap junctions have shown that these channels are relatively selective for cations over anions, suggesting that transfer of other negatively charged molecules through Cx45 channels may also be hindered (23, 37).

Reduced intercellular communication by ROS/Cx45 cells cannot be due to an indirect effect on Cx43 abundance, phosphorylation or localization which were not altered in these cells (Figs. 2–4). Also, our results are not likely to be due to clonal variation, since similar results were obtained with other ROS/Cx45 cell clones.

A possible explanation for altered communication between ROS/Cx45 cells is that transfected Cx45 and native Cx43 directly interact to form mixed gap junction channels. This interaction could occur in two different ways. One possibility is that a homotypic Cx43 hexamer in one cell might bind to a homotypic Cx45 hexamer in another to form a hybrid junction (heterotypic junction). Alternatively, Cx43 and Cx45 might combine in the same cell to form mixed hexamers (heteromeric junction). Formation of heterotypic gap junctions with unique properties has been demonstrated using connexins expressed by *Xenopus* oocytes (1, 8, 16, 33, 38, 39). Specificity of heterotypic gap junction formation in mammalian cells has been demonstrated by Tomasetto et al., who found that Cx26 and Cx43 did not form functional junctions (34).

We found that rat Cx43 and chicken Cx45 can form functional heterotypic gap junction channels using transfected N2A neuroblastoma cells (Li, K., and T. H. Steinberg, unpublished observations). Also, Moreno et al. have shown that heterotypic gap junctions formed by human Cx43 and Cx45 expressed in SKHep1 cells have unitary conductance intermediate between homotypic Cx43 and Cx45 channels (22). Note that heterotypic Cx43/Cx45 channels were impermeant to LY (22).

The possibility that two or more connexins might form a completely mixed heteromeric hemichannel was recently demonstrated by Stauffer (30) using Sf9 cells cotransfected with β-type connexins, Cx32 and Cx26. Assembly of heteromeric channels from α-type connexins has not been demonstrated. One consequence of complete connexin intermixing in ROS/Cx45 cells would be that the molecular permeability of gap junctions in these cells might be determined by the stoichiometry of Cx43 and Cx45. For instance, two different cell lines, UMR cells which are poorly coupled (32) and BWEM cells which are well coupled (19) endogenously express both Cx43 and Cx45.

Both ROS/Cx45 and ROS/Cx45tr cells showed decreased gap junctional conductance as compared to ROS cells, suggesting that both the full-length and truncated forms of chicken Cx45 were interacting with Cx43. ROS/Cx45 cells had higher g_j than ROS/Cx45tr cells, yet dye transfer by ROS/Cx45tr cells was not reduced. This suggests that the COOH-terminal domain of Cx45 affects either connexin channel permeability or the ability of Cx45 to interact with Cx43. Also, the COOH terminus of Cx45 may be involved in regulating the exclusion of negatively charged molecules (37), while the channel diameter could be controlled by other parts of Cx45, such as helical domains.

The reason for enhanced intercellular transfer of microinjected LY by ROS/Cx45tr cells (Fig. 7 *c*) is not clear at present. Transfer of calcein by ROS/Cx45tr cells was comparable to ROS cells as determined with the FACS assay (Figs. 5 and 6). Note that the microinjection assay measures the dispersion of dye from a single source during a 5-min time period, while the FACS assay involves the transfer of dye from multiple sources during a 5-h incubation. Thus, the increased sensitivity of the FACS assay may obscure subtle differences in dye transfer that are detectable by microinjection.

However, there are other important differences between the two assays. For instance, microinjection uses an established monolayer of cells, while the FACS assay measures intercellular transfer between cells that are in the process of attaching to a surface and forming gap junctions. Also, physical contact of an osteoblast with a micropipette induces increases in cytosolic calcium (Geist, S., and T. H. Steinberg, unpublished observations). Perhaps the COOH terminus of Cx45 is involved in calcium-dependent regulation of gap junctional intercellular communication. There is some precedent for a role of the COOH-terminal domain in regulating connexin function; truncated Cx43 mutants are insensitive to cytosol acidification, which normally inhibits Cx43-mediated intercellular communication (12, 20).

In summary, we have found that the expression of one connexin can alter intercellular communication mediated by another connexin. This suggests that in cells expressing multiple connexins, these proteins interact and form gap junctions with properties distinct from those of gap junctions formed by the individual connexins. Additional work will be required to determine whether this is due to heterotypic or heteromeric channel formation. Connexin multiplicity may provide a mechanism that allows the cell to regulate the intercellular permeation of molecules in a manner that would not be possible with the expression of only a single connexin.

This research was supported in part by National Institutes of Health (NIH) grants GM45815 (T. H. Steinberg), DK46686 (T. H. Steinberg), AR41255 (R. Civitelli), HL45466 (E. C. Beyer), and EY08368 (E. C. Beyer), and a grant from the Monsanto/Searle-Washington University Biomedical Research Agreement. M. Koval is an Amgen Fellow of the Life Sciences Research Foundation and was partially supported by an NIH postdoctoral grant. T. H. Steinberg and E. C. Beyer are Established Investigators of the American Heart Association.

Received for publication 28 December 1994 and in revised form 26 April 1995.

References

1. Barrio, L. C., T. Suchyna, T. Bargiello, L. X. Xu, R. S. Roginski, M. V. Bennett, and B. J. Nicholson. 1991. Gap junctions formed by connexins 26 and 32 alone and in combination are differently affected by applied voltage. *Proc. Natl. Acad. Sci. USA.* 88:8410–8414.
2. Bennett, M. V. L., L. C. Barrio, T. A. Bargiello, D. C. Spray, E. Hertzberg, and J. C. Saez. 1991. Gap junctions: new tools, new answers, new questions. *Neuron.* 6:305–320.
3. Beyer, E. C. 1990. Molecular cloning and developmental expression of two chick embryo gap junction proteins. *J. Biol. Chem.* 265:14439–14443.
4. Beyer, E. C., and T. H. Steinberg. 1991. Evidence that the gap junction protein connexin-43 is the ATP-induced pore of mouse macrophages. *J. Biol. Chem.* 266:7971–7974.
5. Beyer, E. C., D. L. Paul, and D. A. Goodenough. 1987. Connexin43: a protein from rat heart homologous to a gap junction protein from liver. *J. Cell Biol.* 105:2621–2629.
6. Beyer, E. C., D. L. Paul, and D. A. Goodenough. 1990. Connexin family of gap junction proteins. *J. Membr. Biol.* 116:187–194.
7. Brisette, J. L., N. M. Kumar, N. B. Gilula, J. E. Hall, and G. P. Dotto. 1994. Switch in gap junction protein expression is associated with selective changes in junctional permeability during keratinocyte differentiation. *Proc. Natl. Acad. Sci. USA.* 91:6453–6457.
8. Bruzzone, R., J. A. Haeflinger, R. L. Gimlich, and D. L. Paul. 1993. Connexin 40, a component of gap junctions in vascular endothelium, is restricted in its ability to interact with other connexins. *Mol. Biol. Cell.* 4:7–20.
9. Carel, J.-C., B. Frazier, T. J. Ley, and V. M. Holers. 1989. Analysis of epitope expression and the functional repertoire of recombinant complement receptor 2 (CR2/CD21) in mouse and human cells. *J. Immunol.* 143: 923–930.
10. Chiba, H., N. Sawada, M. Oyamada, T. Kojima, S. Nomura, S. Ishii, and M. Mori. 1993. Relationship between the expression of the gap junction protein and osteoblast phenotype in a human osteoblastic cell line during cell proliferation. *Cell Struct. Funct.* 18:419–426.
11. Civitelli, R., E. C. Beyer, P. M. Warlow, A. J. Robertson, S. T. Geist, and T. H. Steinberg. 1993. Connexin 43 mediates direct intercellular communication in human osteoblastic cell networks. *J. Clin. Invest.* 91:1888–1894.
12. Ek, J. F., M. Delmar, R. Perzova, and S. M. Taffet. 1994. Role of histidine 95 on pH gating of the cardiac gap junction protein connexin43. *Circ. Res.* 74:1058–1064.
13. Evans, W. H. 1994. Assembly of gap junction intercellular communication channels. *Biochem. Soc. Trans.* 22:788–792.
14. Harlow, E., and D. Lane. 1988. Antibodies. A Laboratory Manual. Cold Spring Harbor Laboratory, Cold Spring Harbor, NY. 636–639.
15. Hertzberg, E. L. 1984. A detergent-independent procedure for the isolation of gap junctions from rat liver. *J. Biol. Chem.* 259:9936–9943.
16. Henneman, H., T. Suchyna, H. Lichtenberg-Frate, S. Jungblut, E. Dahl, H.-J. Schwarz, B. J. Nicholson, and K. Willecke. 1992. Molecular cloning and functional expression of mouse connexin 40, a second gap junction gene preferentially expressed in lung. *J. Cell Biol.* 117:1299–1310.
17. Horan, P. K., M. J. Melnikoff, B. D. Jensen, and S. E. Slezak. 1990. Fluorescent cell labeling for in vivo and in vitro cell tracking. *In* Methods in Cell Biology. Vol. 33. Flow Cytometry. Z. Darzynliewicz and H. A. Crissman, editors. Academic Press, San Diego, CA. 469–490.
18. Kren, B. T., N. M. Kumar, S. Wang, N. B. Gilula, and C. J. Steer. 1993. Differential regulation of multiple gap junction transcripts and proteins during rat liver regeneration. *J. Cell Biol.* 123:707–718.
19. Laing, J. G., E. M. Westphale, G. L. Engelmann, and E. C. Beyer. 1994. Characterization of the gap junction protein, connexin45. *J. Membr. Biol.* 139:31–40.
20. Liu, S., S. Taffet, L. Stoner, M. Delmar, M. L. Vallano, and J. Jalife. 1993. A structural basis for the unequal sensitivity of the major cardiac and liver gap junctions to intracellular acidification: the carboxy tail length. *Biophys. J.* 64:1422–1433.
21. Loewenstein, W. R., and B. Rose. 1992. The cell-cell channel in the control of growth. *Semin. Cell Biol.* 3:59–79.
22. Moreno, A. P., G. I. Fishman, E. C. Beyer, and D. C. Spray. 1995. Voltage dependent gating and single channel analysis of heterotypic gap junction channels formed of Cx45 and Cx43. *Prog. Cell Res.* 4:405–410.
23. Moreno, A. P., J. G. Laing, E. C. Beyer, and D. C. Spray. 1995. Properties of gap junction channels formed of connexin 45 endogenously expressed in human hepatoma (SKHep1) cells. *Am. J. Physiol.* 268(*Cell Physiol.* 37):C356–C365.
24. Musil, L. S., and D. A. Goodenough. 1991. Biochemical analysis of connexin 43 intracellular transport, phosphorylation, and assembly into gap junctional plaques. *J. Cell Biol.* 115:1357–1374.
25. Musil, L. S., and D. A. Goodenough. 1993. Multisubunit assembly of an integral plasma membrane channel protein, gap junction connexin 43, occurs after exit from the ER. *Cell.* 74:1065–1077.
26. Schiller, P. C., P. P. Mehta, B. A. Roos, and G. A. Howard. 1992. Hormonal regulation of intercellular communication: parathyroid hormone increases connexin 43 gene expression and gap-junctional communication in osteoblastic cells. *Mol. Endocrinol.* 6:1433–1440.
27. Schirrmacher, K., I. Schmitz, E. Winterhager, O. Traub, F. Brummer, D. Jones, and D. Bingmann. 1992. Characterization of gap junctions between osteoblast-like cells in culture. *Calcif. Tissue Int.* 51:285–290.
28. Shen, V., L. Rifas, G. Kohler, and W. A. Peck. 1986. Prostaglandins change cell shape and increase intercellular gap junctions in osteoblasts cultured from rat fetal calvaria. *J. Bone Miner. Res.* 1:243–249.
29. Sokal, R. R., and F. J. Rohlf. 1981. Biometry. 2nd Ed. W. H. Freeman & Co., New York, NY. pp. 433–445.
30. Stauffer, K. A. 1995. The gap junction proteins β_1-connexin (connexin32) and β_2-connexin (connexin26) can form heteromeric hemichannels. *J. Biol. Chem.* 270:6768–6772.
31. Stauffer, K. A., and N. Unwin. 1992. Structure of gap junction channels. *Semin. Cell Biol.* 3:17–20.
32. Steinberg, T. H., R. Civitelli, S. T. Geist, A. J. Robertson, E. Hick, R. D. Veenstra, H.-Z. Wang, P. M. Warlow, E. M. Westphale, J. G. Laing, et al. 1994. Connexin 43 and connexin 45 form gap junctions with different molecular permeabilities in osteoblastic cells. *EMBO (Eur. Mol. Biol. Organ.) J.* 13:744–750.
33. Swenson, K. I., J. R. Jordan, E. C. Beyer, and D. L. Paul. 1989. Formation of gap junctions by expression of connexins in Xenopus oocyte pairs. *Cell.* 57:145–155.
34. Tomasetto, C., M. J. Neveu, J. Daley, P. K. Horan, and R. Sager. 1993. Specificity of gap junction communication among human mammary cells and connexin transfectants in culture. *J. Cell Biol.* 122:157–167.
35. Veenstra, R. D. 1990. Voltage-dependent gating of gap junction channels in embryonic chick ventricular cell pairs. *Am. J. Physiol.* 258:C662–C672.
36. Veenstra, R. D., H.-Z. Wang, E. M. Westphale, and E.C. Beyer. 1992. Multiple connexins confer distinct regulatory and conductance properties of gap junctions in developing heart. *Circ. Res.* 71:1277–1283.
37. Veenstra, R. D., H.-Z. Wang, E. C. Beyer, and P. R. Bunk. 1994. Selective dye and ionic permeability of gap junctions formed by connexin 45. *Circ. Res.* 75:483–490.
38. Werner, R., E. Levine, C. Rabadan-Diehl, and G. Dahl. 1989. Formation of hybrid channels. *Proc. Natl. Acad. Sci. USA.* 86:5380–5384.
39. White, T. W., R. Bruzzone, S. Wolfram, D. L. Paul, and D. A. Goodenough. 1994. Selective interactions among the multiple connexin proteins expressed in the vertebrate lens: the second extracellular domain is a determination of compatibility between connexins. *J. Cell Biol.* 125: 879–892.
40. Willecke, K., H. Hennemann, E. Dahl, and S. Jungbluth. 1993. The mouse connexin gene family. *In* Progress in Cell Research. Vol 3. J. E. Hall, G. A. Zampighi, and R. M. Davis, editors. Elsevier Science Publishers, Amsterdam. pp. 33–37.